Supporting Information

Eliminating Low-Crystalline Defects in Spent Graphite Anodes via Low-Temperature Molten Salt Activation and Controlled Oxidation

Zikun Mai[a,b], Yuhao Ge[a,b], Yuan Feng[b], Kai Luo[b], Hao Zhang[b], Meng Huang*[a,b], Jiashen Meng*[b,c,e], Xuanpeng Wang*[a,c,d,e]

a. *Sanya Science and Education Innovation Park, Wuhan University of Technology, Sanya 572000, China.*
b. *State Key Laboratory of Advanced Technology for Materials Synthesis and Processing, School of Materials Science and Engineering, Wuhan University of Technology, Wuhan 430070, China.*
c. *Hubei Longzhong Laboratory, Wuhan University of Technology (Xiangyang Demonstration Zone), Xiangyang 441000, China.*
d. *Department of Physical Science and Technology, School of Physics and Mechanics, Wuhan University of Technology, Wuhan 430070, China.*
e. *Zhongyu Feima New Material Technology Innovation Center (Zhengzhou) Co., Ltd., Zhengzhou 450001, China.*
f. Supplementary Information available: [details of any supplementary information available should be included here]. See DOI: 10.1039/x0xx00000x

The calculation of lithium-ion diffusion coefficient (D_{Li^+}):

$$I_p = 269000n^{3/2}ACD^{1/2}V^{1/2} \quad (1)$$

$$k = I_p/V^{1/2} \quad (2)$$

$$D_{Li^+} = \left(\frac{k}{269000n^{3/2}AC}\right)^2 \quad (3)$$

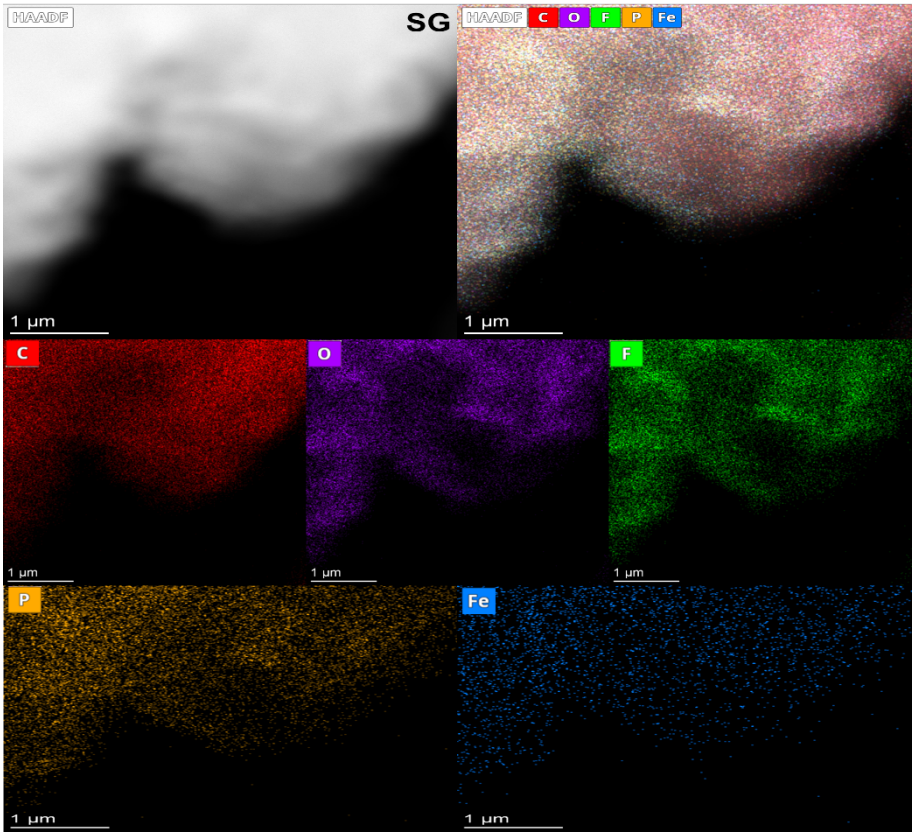

Fig. S1. TEM energy spectrum characterization of SG.

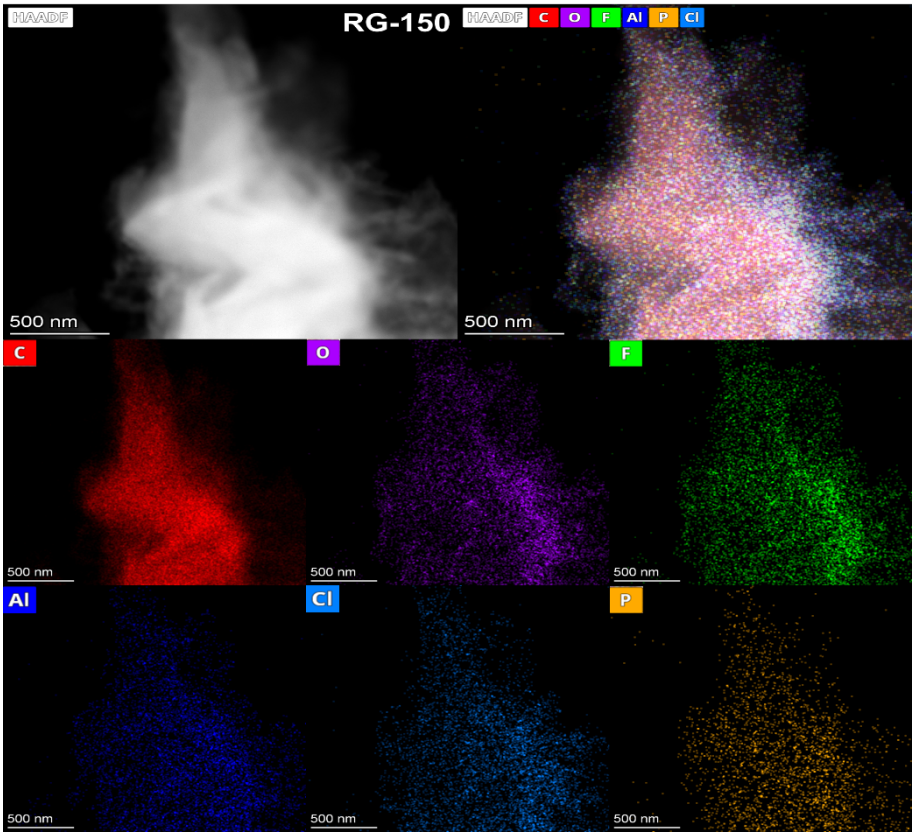

Fig. S2. TEM energy spectrum characterization of RG-150.

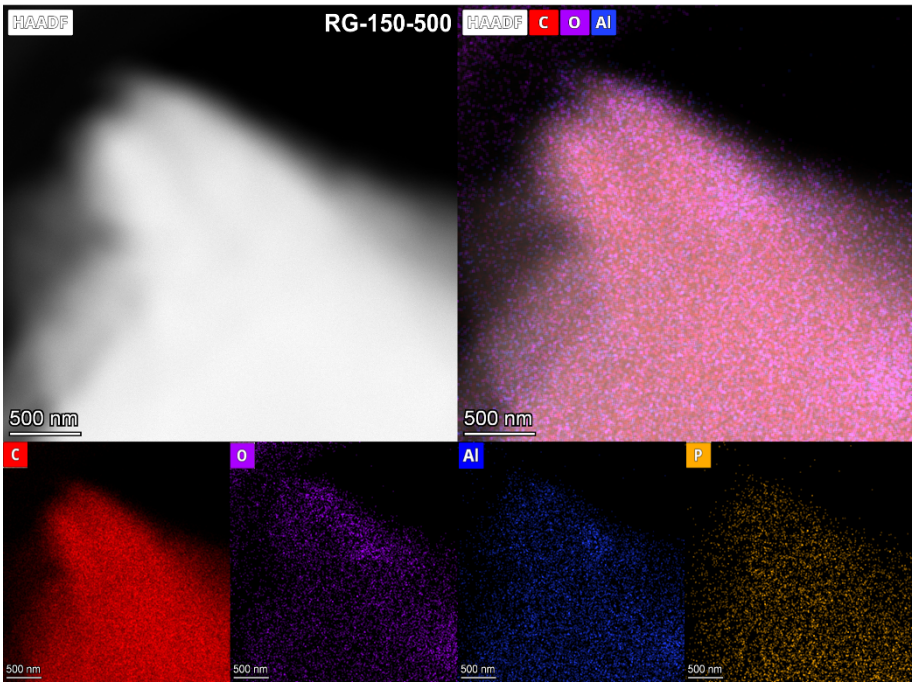

Fig. S3. TEM energy spectrum characterization of RG-150-500.

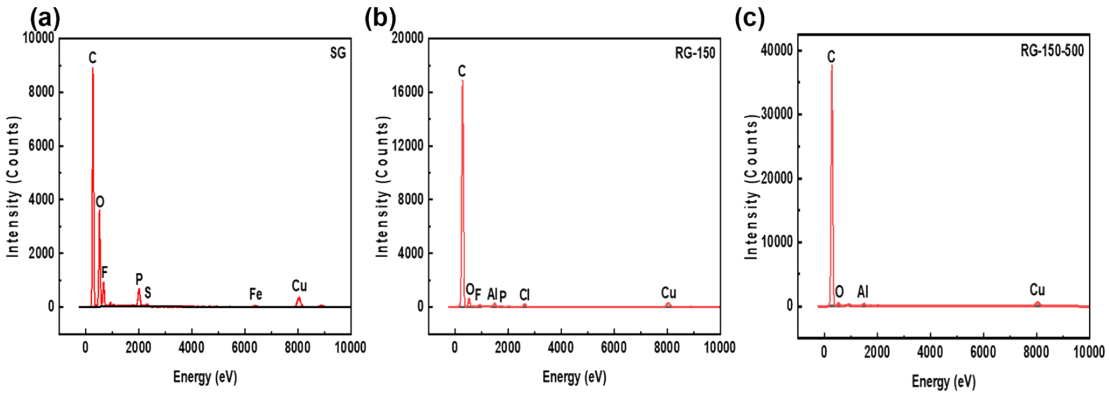

Fig. S4. TEM elemental spectrum of (a) SG, (b) RG-150, and (c) RG-150-500.

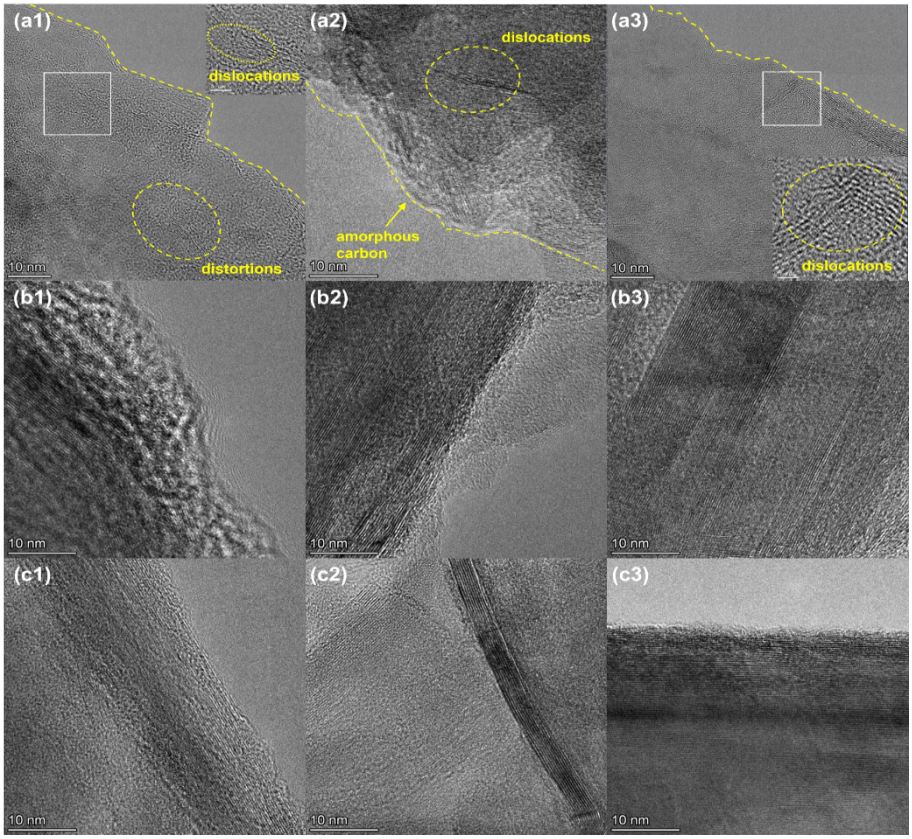

Fig. S5. Lattice stripes at different positions of SG (a1-a3), RG-150 (b1-b3), and RG-150-500 (c1-c3).

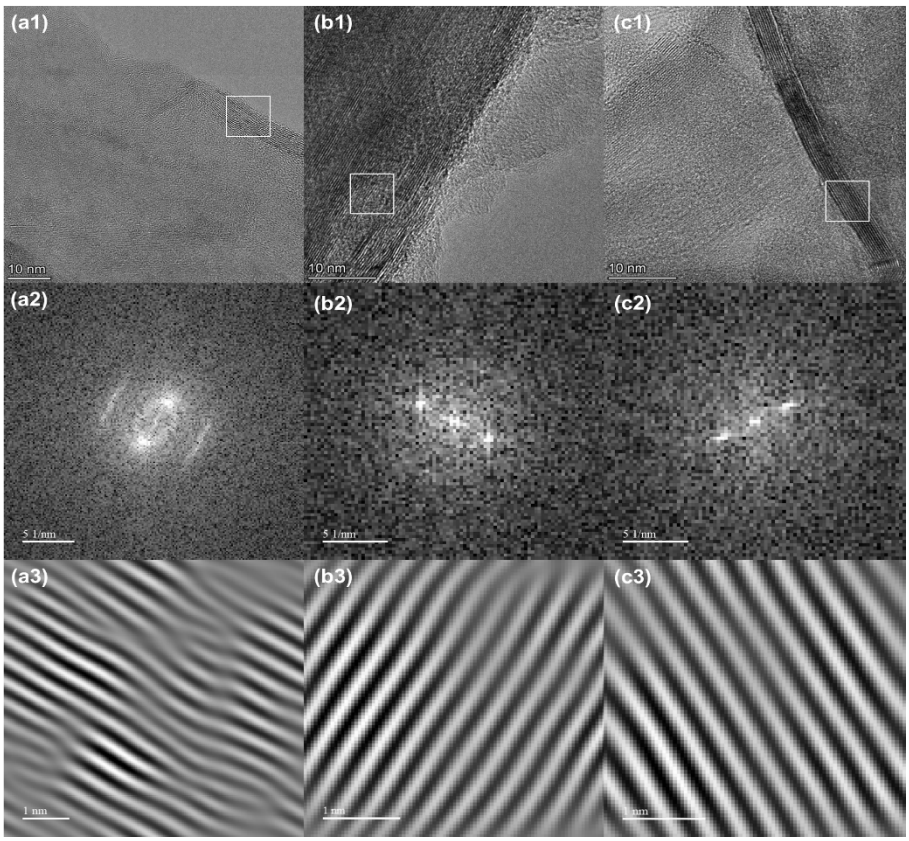

Fig. S6. Lattice stripes and FFT of SG (a1-a3), RG-150 (b1-b3), and RG-150-500 (c1-c3).

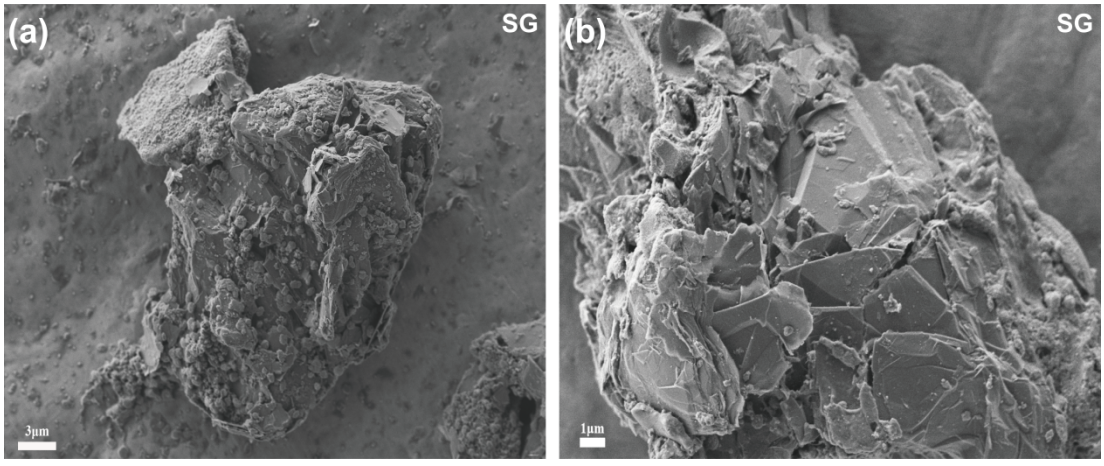

Fig. S7. SEM images of SG.

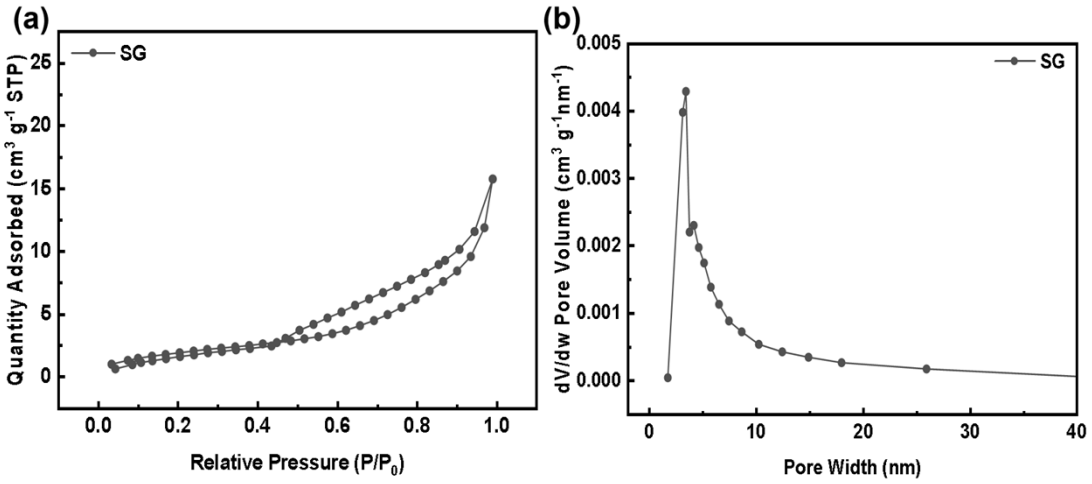

Fig. S8. (a) Nitrogen adsorption-desorption isotherms and (b) pore size distribution of SG.

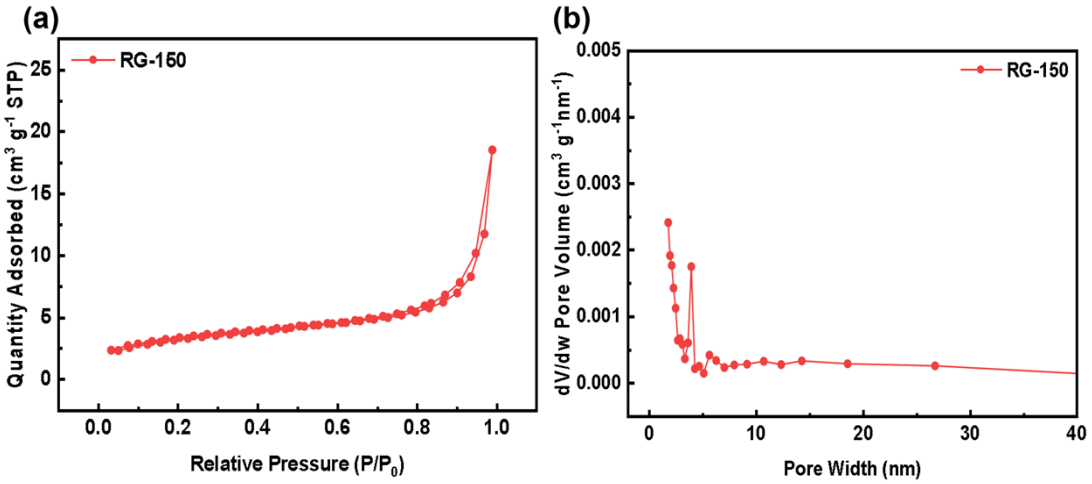

Fig. S9. (a) Nitrogen adsorption-desorption isotherms and (b) pore size distribution of RG-150.

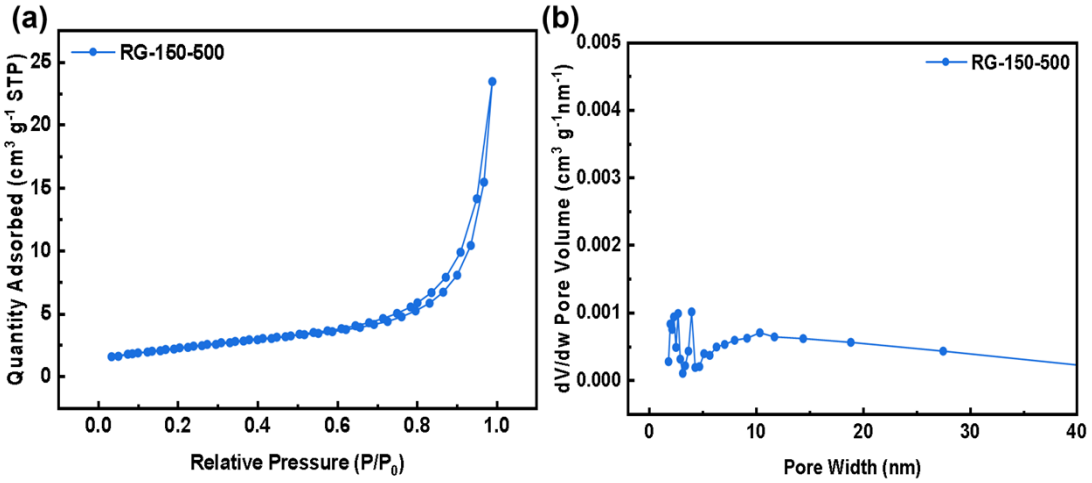

Fig. S10. (a) Nitrogen adsorption-desorption isotherms and (b) pore size distribution of RG-150-500.

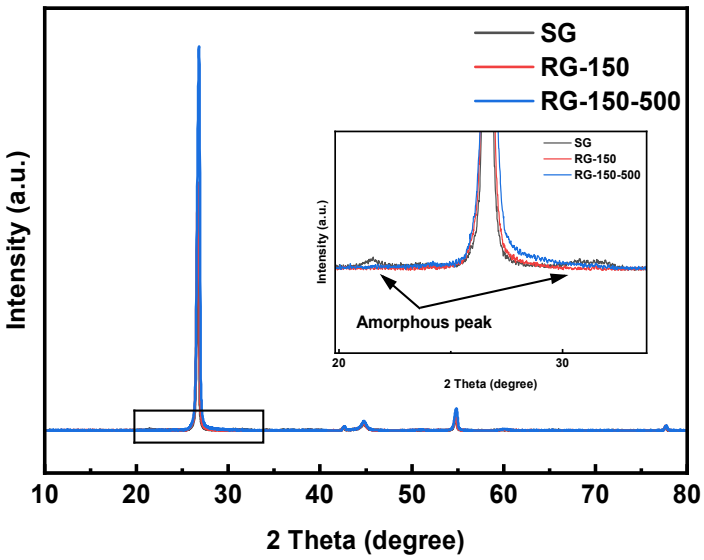

Fig. S11. The XRD patterns of SG, RG-150, and RG-150-500 samples.

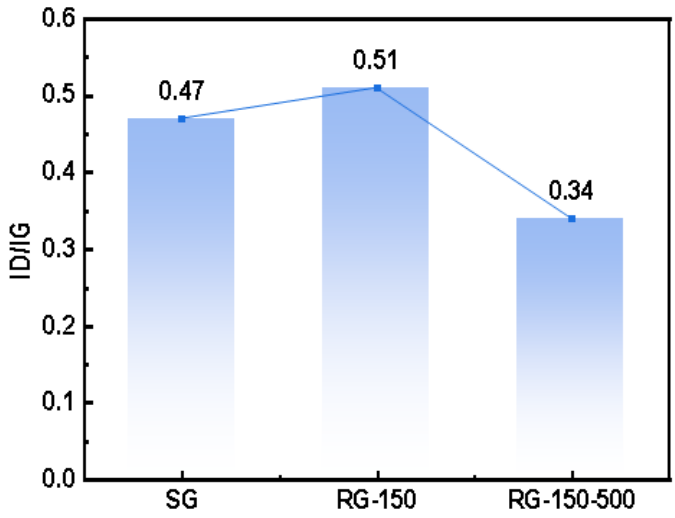

Fig. S12. Comparison of I_D/I_G values for SG, RG-150, and RG-150-500.

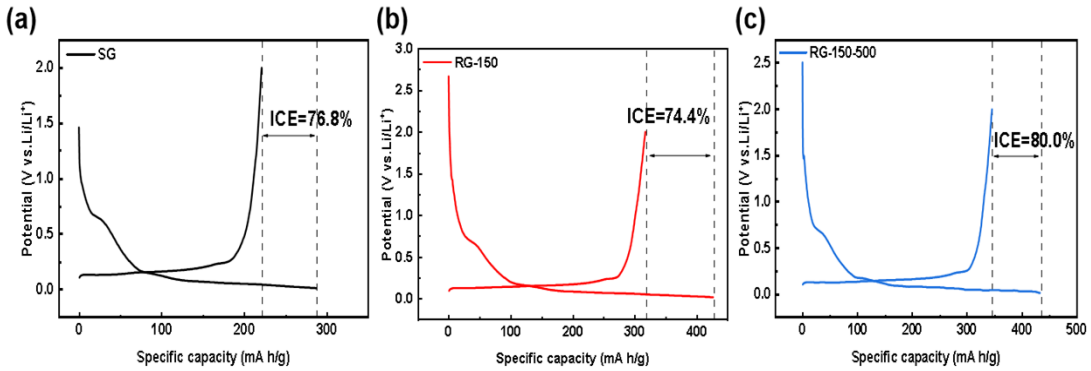

Fig. S13. The initial charging/discharging profiles of (a) SG, (b) RG-150, and (c) RG-150-500 at 0.2C.

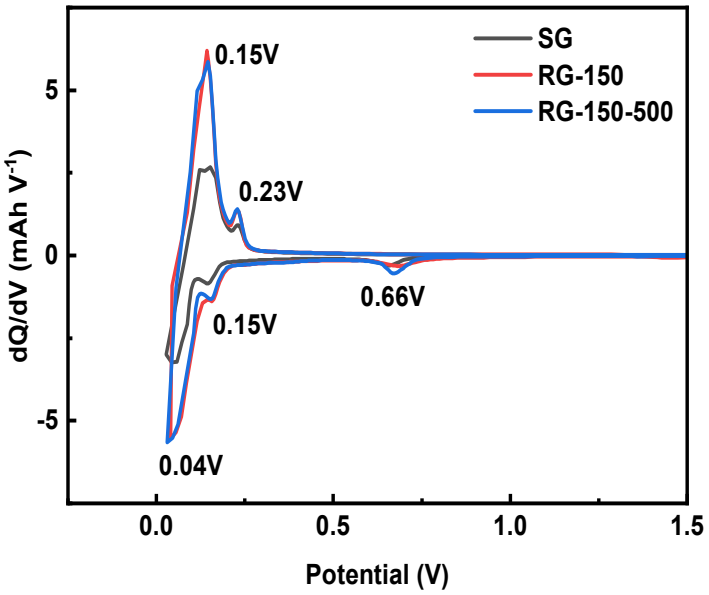

Fig. S14. dQ/dV curves of SG, RG-150, and RG-150-500 during first cycle at 0.2C.

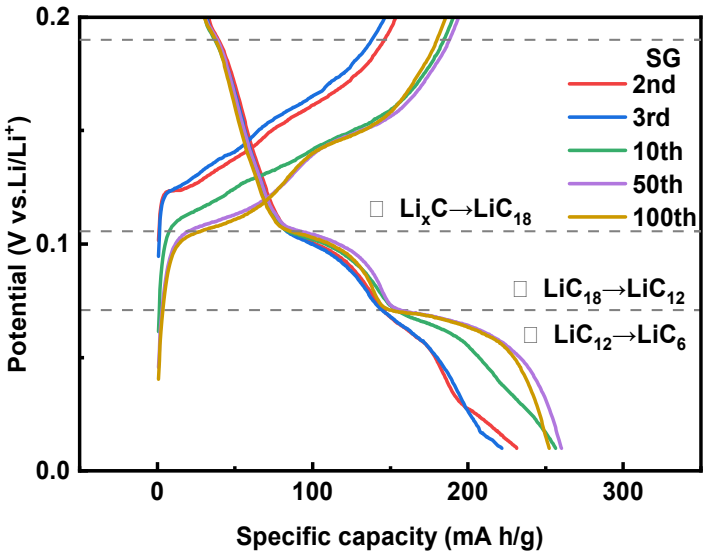

Fig. S15. The constant current charge-discharge curve of SG from 0 to 0.2V at 0.2C.

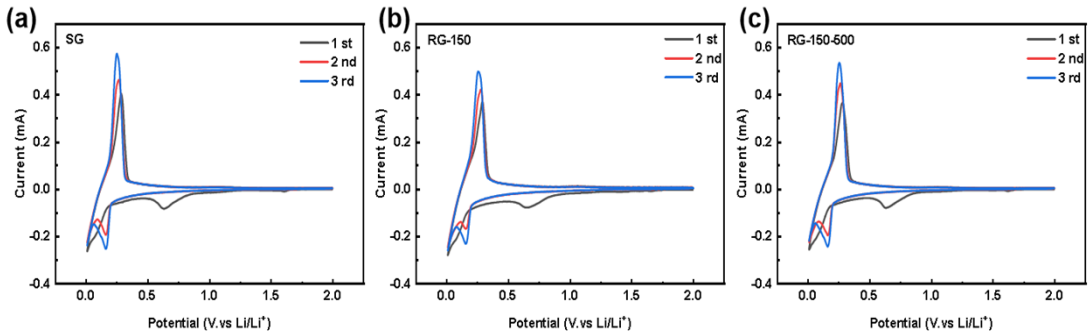

Fig. S16. CV curves for the first three cycles of (a) SG, (b) RG-150, and (c) RG-150-500.

Table S1. EA test results of SG, RG-150, and RG-150-500.

Sample	C (at%)	H (at%)	N (at%)	S (at%)
SG	87.82	11.92	0.14	0.08
RG-150	94.27	5.55	0.13	0.05
RG-150-500	96.04	3.80	0.13	0.03

Table S2. ICP-OES test results of SG, RG-150, and RG-150-500.

Sample	Li (ppm)	P (ppm)	Fe (ppm)
SG	54.624	16.771	3.673
RG-150	0.409	2.774	0.780
RG-150-500	0.194	1.788	0.398

Table S3. Comparison of element content by TEM-EDS.

Sample	C (at%)	O (at%)	F (at%)	P (at%)	S (at%)	Fe (at%)	Al (at%)	Cl (at%)	Si (at%)
SG	74.81	17.54	3.74	2.06	0.18	0.16	/	/	/
RG-150	95.99	1.97	0.16	0.04	0.02	/	0.51	0.40	0.09
RG-150-500	98.33	0.62	/	0.05	/	/	0.24	/	0.03

Table S4. BET test for different graphite powders.

Sample	Surface area (m^2/g)	Pore Size (nm)
SG	8.82	3.44
RG-150	11.44	3.92
RG-150-500	8.14	3.96

Table S5. The positions and intensities of the first five main peaks of SG, RG-150, and RG-150-500 through the PDF method.

		SG	RG-150	RG-150-500
First peak	Position (Å)	1.44	1.44	1.44
	Intensity ($Å^{-2}$)	5.97	7.33	8.46
Second peak	Position (Å)	2.46	2.46	2.46

	Intensity ($Å^{-2}$)	6.76	6.95	8.42
Third peak	Position (Å)	3.72	3.70	3.72
	Intensity ($Å^{-2}$)	5.25	5.68	6.45
Forth peak	Position (Å)	4.26	4.20	4.26
	Intensity ($Å^{-2}$)	5.27	5.58	6.60
Fifth peak	Position (Å)	5	5	5
	Intensity ($Å^{-2}$)	6.78	8.08	9.98

Table S6. Intensity data of Raman by Origin fitting.

Sample	I_D (D-band area)	I_G (G-band area)	I_D/I_G	R^2
SG	3062.4813	6577.7231	0.4656	0.9429
RG-150	13225.5790	25972.4602	0.5092	0.9778
RG-150-500	11807.4176	34252.6789	0.3447	0.9473

Table S7. The influence of defects on the electrochemical properties of graphite.

Sample	C-F	C=O	C-C	1C (mAh g^{-1})	0.2C (mAh g^{-1})	ICE (1C)	ICE (0.2C)
SG	15.3%	18.6%	31.7%	152.5	287.9	64.6%	76.8%
RG-150	7.8%	18.3%	39.7%	342.3	426.9	71.3%	74.4%
RG-150-500	6.9%	8.0%	50.5%	399.4	434.2	81.0%	80.0%

Table S8. The influence of graphite purity (TEM-EDS) on electrochemical performance.

Sample	C (at%)	1C (mAh g^{-1})	After 250 cycles	ICE (1C)	0.2C (mAh g^{-1})	After 250 cycles	ICE (0.2C)
SG	74.81	152.5	212.2	64.6%	287.9	232.9	76.8%
RG-150	95.99	342.3	232.0	71.3%	426.9	259.0	74.4%
RG-150-500	98.33	399.4	316.5	81.0%	434.2	360.8	80.0%

Table S9. Comparison of electrochemical properties of recycled graphite

Method	Performance	Ref.
H_2SO_4 curing-calcination at 1500 °C	The initial charge capacity is 349 mAh g^{-1} at 0.1C	[1]

H_2SO_4-H_2O_2 leaching combined with NaOH calcination	discharge capacity of 377.3 mAh g^{-1} at 0.1 C, and 359.3 mAh g^{-1} at 0.2C	2
H_2SO_4 leaching combined with $Co(NO_3)_2$ catalyze	Initial discharging capacity of 358 mAh g^{-1} at 0.1C	3
Calcination from 2000 ^oC to 2800 ^oC	Initial discharging capacity of 346.3 mAh g^{-1} at 0.1C	4
ammonium fluoride roasting and water leaching	Initial discharging capacity of 340.9 mAh g^{-1} at 0.1C	5
KOH-NaOH composite alkali etching	Initial discharging capacity of 320-340 mAh g^{-1} at 0.1C	6
HCl leaching combined with asphalt coating	discharging capacity of 355 mAh g^{-1} at 1C	7
Reconstruction of layered carbon coating using magnesium catalyst at 900 ^oC	Initial discharging capacity of 398 mAh g^{-1} at 0.1C	8
LTMS-calcination	Initial discharge capacity of 399.4 mAh g^{-1} at 1C, and 434.2 mAh g^{-1} at 0.2C	Our work

Table S10. Fitting data of pre cycle electrical impedance spectroscopy (EIS) test.

Sample	SG	RG-150	RG-150-500
Rs(Ω)	8.269	7.572	7.759
Rct(Ω)	387.06	192.90	160.50

Table S11. Fitting data of electrical impedance spectroscopy (EIS) test after 200 cycles.

Sample	SG	RG-150	RG-150-500
Rs(Ω)	8.938	5.851	5.719
Rct(Ω)	22.162	18.296	15.154
R_{SEI}(Ω)	5.709	6.777	4.923

Table S12. Total cost of recycled graphite

	Hydrometallurgy	Pyrometallurgy(2000-3000˚C)	LTMS-calcination	Data source
Materials cost ($/kg)	3.753	0	0.897	CB

Energy cost ($/kg)	4.463	9.563	6.545	ISM、BD
Total cost ($/kg)	8.216	9.563	7.442	
Profit ($/kg)	1.784	0.437	2.558	

Hydrometallurgy:

It was soaked with 5 M sulfuric acid and 35 w/w % H_2O_2 at room temperature. The mixture was stirred in a beaker with a mechanical stirrer for 1 hour. Subsequently, the mixture was taken out, and calcination experiments were carried out in a tube furnace. The roasted material was leached in sulfuric acid solution. Then centrifuged, washed, and dried. Finally, the graphite after re-leaching treatment was sintered with NaOH powder at 500 ˚C for 2 h, washed with DI water, and dried again.

Energy consumption of mechanical agitators: 0.5 kW* 1 h = 0.5 kW h
Energy consumption of tube furnace: 6 kW * 4 h + 6 kW * 2 h = 36 kW h
Energy consumption of the drying oven: 1 kW * 8 h + 1 kW * 8 h= 16 kW h
Total energy cost: (0.5+36+16) kW h * $ 0.085 kWh^{-1} ≈ $ 4.4625
CB: https://www.chemicalbook.com/. ISM: https://www.instrument.com.cn
BD: https://www.baidu.com/

Pyrometallurgy:

The obtained spent graphite samples (SG) were heat-treated in a tube furnace at 500 ˚C for 4 hours, and impurities were removed by washing and drying. The SG was then ground using a planetary ball mill until it passed a 400 mesh sieve. The samples were placed in a tube furnace for the heat treatment process under an Ar atmosphere. The samples were individually heated to 2800 ˚C, kept at that temperature for 12 h, and cooled to room temperature to obtain regenerated graphite (RG).

Energy consumption of tube furnace : 6 kW * 4 h + 6 kW * 12 h = 96 kW h
Energy consumption of the drying oven: 1 kW * 12 h = 12 kW h
Energy consumption of ball mill: 0.75 kW* 6 h = 4.5 kW h
Total energy cost: (96+12+4.5) kW h * $ 0.085 kWh^{-1} ≈ $ 9.5625

LTMS-calcination:
Muffle Furnace Energy Consumption: 2.5 kW * 24 h + 2.5 kW * 2 h = 65 kW h
Energy consumption of the drying oven: 1 kW * 12 h = 12 kW h
Total energy cost: (65+12) kW h * $ 0.085 kWh^{-1} ≈ $ 6.545

References

1. Y. Gao, C. Wang, J. Zhang, Q. Jing, B. Ma, Y. Chen and W. Zhang, *ACS Sustainable Chemistry & Engineering*, 2020, **8**, 9447-9455.
2. X. Ma, M. Chen, B. Chen, Z. Meng and Y. Wang, *ACS Sustainable Chemistry & Engineering*, 2019, **7**, 19732-19738.
3. Q. Chen, L. Huang, J. Liu, Y. Luo and Y. Chen, *Carbon*, 2022, **189**, 293-304.
4. G.-Q. Yu, M.-Z. Xie, Z.-H. Zheng, Z.-G. Wu, H.-L. Zhao and F.-Q. Liu, *Resources, Conservation and Recycling*, 2023, **199**, 107267.
5. X. Zhu, J. Xiao, Q. Mao, Z. Zhang, Z. You, L. Tang and Q. Zhong, *Chemical Engineering Journal*, 2022, **430**, 132703.
6. H. Da, M. Gan, D. Jiang, C. Xing, Z. Zhang, L. Fei, Y. Cai, H. Zhang and S. Zhang, *ACS Sustainable Chemistry & Engineering*, 2021, **9**, 16192-16202.
7. K. Chen, Y. Ding, L. Yang, Z. Wang, H. Yu, D. Fang, Y. Feng, L. Hu, C. Xu, P. Shao, X. Luo and L. Chen, *Resources, Conservation and Recycling*, 2024, **201**, 107326.
8. S. Luo, F. Liu, W. Tianxu, Y. Liu, C. Zhang, C. Bie, M. Liu, P. K. Chu, K. Huo and B. Gao, *Energy Storage Materials*, 2024, **73**, 103833.